Computer simulations of bent-core liquid crystals

Computer simulations of bent-core liquid crystals

Alastair Dewar and Philip J. Camp*
School of Chemistry, The University of Edinburgh, West Mains Road, Edinburgh EH9 3JJ, United Kingdom
(Received 29 December 2003; published 15 July 2004)

The phase behavior of model linear and bent-core molecules has been studied using isothermal-isobaric Monte Carlo computer simulations. The molecular model consists of seven Lennard-Jones spheres rigidly arranged in a "V" shape, with external bond angle, γ. With $\gamma=0°$ (linear molecules), we find isotropic, nematic, untilted smectic *A*, and two layered phases in which the molecules are tilted with respect to the layer normal. The latter two phases correspond to distinct branches in the equation of state, and possess different types of ordering within and between the layers; these phases are tentatively assigned as being smectic *B* and crystal. Apart from the possible existence of a tilted smectic *B*, the phase behavior of this system is broadly in line with earlier simulation studies on related linear molecular models. In the $\gamma=20°$ system, isotropic, nematic, and tilted smectic-*B* phases are observed. Interestingly, the range of stability of the nematic phase is enhanced compared to the $\gamma=0°$ system. In simulations of the $\gamma=40°$ system, nematic phases are absent, and only isotropic and tilted phases are in evidence. The in-layer structure of the tilted phases shows a very clear change from smectic-*B* to smectic-*A* ordering upon increasing the temperature. In all instances of a tilted phase, the degree of molecular tilt is in the region of $30\pm5°$, with respect to the smectic layer normal, which corresponds closely to typical experimental observations in real bent-core liquid crystals. In our model, the tilt provides efficient packing of the spheres and favorable attractive interactions between molecules. The relevance of the present simulation model to real bent-core liquid crystals is discussed critically.

DOI: 10.1103/PhysRevE.70.011704 PACS number(s): 61.30.Cz, 64.70.Md

I. INTRODUCTION

The emergence of a new class of liquid crystalline materials was signaled by the synthesis of achiral bent-core molecules that are able to form chiral ferroelectric or antiferroelectric smectic phases [1]. Typically, the molecules are of C_{2v} symmetry, and often possess a permanent electric dipole moment parallel to the principal molecular (C_2) symmetry axis. A typical example of a bent-core molecule is shown in Fig. 1. The substituents ("R" in Fig. 1) are usually either simple alkyl (C_nH_{2n+1}) [1] or alkoxy (OC_nH_{2n+1}) [2] groups.

In biaxial smectic phases, the dipoles are preferentially oriented perpendicular to the layer normal, largely as a result of the molecular biaxiality and the way in which the molecules pack. The formation of ferroelectric and antiferroelectric phases is also seen to be accompanied by the molecules being tilted with respect to the layer polarizations. Therefore, ferroelectric and antiferroelectric phases may exhibit chiral order if the molecules within each layer are tilted in the same sense with respect to the layer polarizations [1–3].

To date, several models of rigid bent-core molecules have been studied using Monte Carlo (MC) and molecular dynamics (MD) computer simulations. In the work summarized below, the molecules possess C_{2v} symmetry, with the "steric" or actual dipole parallel with the C_2 symmetry axis. In what follows, whether the molecules carry an electric dipole or not, the terms ferroelectric, antiferroelectric, superparaelectric, and paraelectric will be used to describe the ordering of the molecular C_2 axes and the layer polarizations in smectic and crystalline phases: ferroelectric means all C_2 axes and layer polarizations are aligned; antiferroelectric means that the polarizations of neighboring smectic layers are antiparallel; superparaelectric means that although the layers are polarized, there is a random distribution of polarization directions in the plane of the layers; and finally, paraelectric denotes a disordered distribution of the C_2 axes, i.e., the layers are not individually polarized. In addition, in tilted ferroelectric and antiferroelectric phases, synclinic ordering means that molecules in neighboring layers are tilted in the same direction with respect to the layer normal, whereas anticlinic ordering means that the molecules in neighboring layers are tilted in opposite directions.

The phase behavior of hard-spherocylinder dimers was studied in preliminary work by Camp *et al.* [4], and more thoroughly by Lansac *et al.* [5]. Referring to this latter work, isotropic, uniaxial nematic, paraelectric smectic-*A*, antiferroelectric smectic-*A*, columnar, paraelectric crystalline, and antiferroelectric crystalline phases were found. In neither of these studies were tilted phases in evidence. Lansac *et al.* also examined the relative thermodynamic stabilities of ferroelectric and antiferroelectric smectic-*A* phases [5]. For dimers with an external bond angle of $\gamma=60°$, and at a packing fraction of about 0.45, the antiferroelectric phase was calculated to be $(0.0035\pm0.0002)k_BT$ lower in Gibbs free energy than the ferroelectric phase. This can be rationalized using a "sawtooth model" in which the molecules in neighboring layers can partially interdigitate in the antiferroelectric phase, but not in the ferroelectric phase.

Continuous potentials studied to date include Gay-Berne dimers [6–8], and site-site molecular models made up of purely repulsive soft spheres [9]. Memmer carried out constant-pressure Monte Carlo (*NpT*-MC) simulations of Gay-Berne dimers with external bond angle $\gamma=40°$, in a

*Electronic address: philip.camp@ed.ac.uk

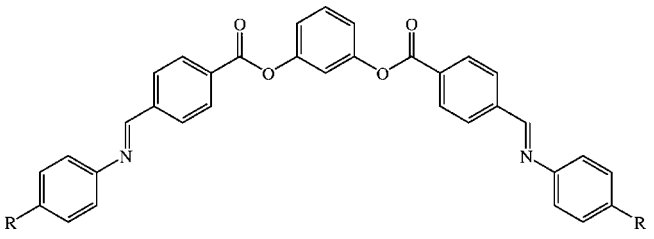

FIG. 1. A typical example of a bent-core molecule [1].

cuboidal simulation cell with independently varied box lengths [6]. These simulations showed nematic and untilted antiferroelectric smectic phases, and a chiral helical superstructure close to the nematic-smectic transition temperature. *NpT*-MD simulations of a similar Gay-Berne model with varying external bond angles in the range $0° \leqslant \gamma \leqslant 70°$ were carried out by Johnston *et al.* [7]. These simulations were performed in a cuboidal box with fixed aspect ratio 1:1:2. With $\gamma = 0°$, isotropic, nematic, smectic-*A*, and smectic-*B* phases were found. With a modest amount of molecular bend ($\gamma = 10°$), the nematic phase was seen to disappear, resulting in a direct isotropic-smectic transition. Upon increasing the bond angle further to $\gamma = 20°$, the nematic phase was reinstated, and a tilted smectic-*B* phase was observed. An interesting twisted grain-boundary (TGB) phase was discovered in a system with $\gamma = 40°$, while at a quite extreme molecular geometry ($\gamma = 70°$), no ordered phases were observed. Johnston *et al.* have also carried out a simulation study of the same bent-core molecular model, but with a transverse dipole moment along the C_2 molecular axis [8]. It was seen that with moderate bond angles ($\gamma \leqslant 40°$) the additional dipole-dipole interactions destabilize the uniaxial nematic phase, and favor the formation of a synclinic antiferroelectric smectic phase.

A site-site bent-core model made up of seven soft spheres interacting via a Weeks-Chandler-Andersen repulsive potential was studied by Xu *et al.* [9]. Monte Carlo simulations of this model were carried out in the canonical (*NVT*) ensemble, using a cuboidal cell of variable shape containing four smectic layers. With an external bond angle $\gamma = 40°$, a tilted paraelectric crystalline phase was found that undergoes a transition to a paraelectric smectic-*A* phase as the temperature is raised, or the density is lowered. The stability of the tilted phase was attributed to a favorable close packing of the spheres on neighboring molecules made possible by the molecular tilt.

From the work that has appeared to date, it should be clear that dipole-dipole interactions are not necessary in the formation of tilted smectic phases. On the other hand, it is obvious that dipolar forces would help stabilize antiferroelectric phases, since the lowest-energy configuration of neighboring layer polarizations is antiparallel; this has been demonstrated in the work on polar Gay-Berne molecules by Johnston *et al.* [8]. The formation of smectic phases of bent-core molecules with polarized layers is, therefore, driven largely by the molecular shape. With the exception of the composite soft-sphere model studied by Xu *et al.* [9], however, the models listed above are all dimer models. Although a great deal can be learned about the fundamental properties of condensed phases from such simple molecular models, it could be argued that a multisite model is more appropriate in the case of bent-core compounds. Attractive interactions might also be included in models of thermotropic liquid crystals; these are omitted from the model studied by Xu *et al.* [9].

With these comments in mind, we set out to study a family of model bent-core molecules that may provide a more faithful representation of the essential molecular characteristics of real compounds. The molecular model consists of seven Lennard-Jones (LJ) spheres arranged in a "V" formation with external bond angle γ, as illustrated in Fig. 2. We have investigated three bond angles, $\gamma = 0°$, $\gamma = 20°$, and $\gamma = 40°$. Assuming that the relative locations of the aryl groups largely dictate the molecular geometry, the molecule as illustrated in Fig. 1 would have an external bond angle closer to $\gamma = 60°$. It should be remembered, however, that there are intramolecular rotations that can reduce this figure considerably, and that in condensed phases, particular conformations may be thermodynamically favored if they lead to improved packing or energetic stabilization. Another factor is the orientation of the alkyl or alkoxy tail groups, which can influence the effective molecular elongation and degree of molecular nonlinearity. Experimental measurements indicate that γ is usually in the range $20° - 40°$, at least in condensed phases, and so the range of molecular bond angles studied in this work is physically relevant. We note that Paolini *et al.* have studied a similar model of linear molecules made up of 11 purely repulsive soft spheres [10]; they found isotropic, nematic, smectic-*A*, and crystalline chevron (tilted) phases. Galindo *et al.* have recently reported a simulation study of the vapor, isotropic liquid, and solid phases of linear molecules made up of three and five Lennard-Jones spheres [11]; however, no liquid-crystalline phases were observed in this work.

In the present model, the total configurational energy U of the system is given by a sum over all pairs of spheres on different molecules

$$U = \sum_{i=1}^{N_m} \sum_{j>i}^{N_m} \sum_{k=1}^{N_s} \sum_{l=1}^{N_s} u(|\mathbf{r}_{ik} - \mathbf{r}_{jl}|), \tag{1}$$

where N_m is the total number of molecules, $N_s = 7$ is the number of spheres per molecule, and $\mathbf{r}_{ik}$ is the position vector of the kth sphere on the ith molecule. $u(r)$ is the sphere-sphere potential, which in this work we take to be the LJ $(12,6)$ potential,

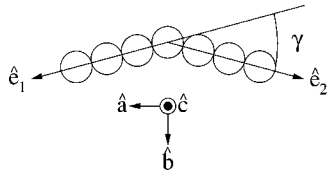

FIG. 2. The composite Lennard-Jones molecule (CLJM). $\hat{\mathbf{e}}_1$ and $\hat{\mathbf{e}}_2$ are unit vectors representing the orientations of the two "arms" of the molecule. The molecular frame is specified by the unit vectors $\hat{\mathbf{a}}$, $\hat{\mathbf{b}}$, and $\hat{\mathbf{c}}$ defined in Eqs. (4)–(6).

$$u(r) = \begin{cases} 4\epsilon\left[\left(\frac{\sigma}{r}\right)^{12} - \left(\frac{\sigma}{r}\right)^{6}\right] & r \leqslant r_{\mathrm{cut}} \\ 0 & r > r_{\mathrm{cut}} \end{cases}, \qquad (2)$$

where r is the pair separation, ϵ is the potential-well depth, σ is the LJ sphere diameter, and $r_{\mathrm{cut}}=2.5\sigma$. Neighboring spheres on a given molecule are separated by a distance equal to 1σ. This part of the model represents the fairly rigid bent core of real molecules (cf. Fig. 1); for brevity we refer to these model molecules as composite LJ molecules (CLJMs).

In this paper we report the results of *NpT*-MC simulations of CLJMs carried out to explore the phase behavior. We will show that this molecular model is sufficient to simulate the formation of nematic and tilted smectic phases. Moreover, we confirm that the main driving force for the formation of tilted phases is the favorable interactions arising from the "close packing" of spheres on neighboring molecules. We argue that this scenario is physically relevant, bearing in mind that many real bent-core molecules are often made up of several aryl groups (see Fig. 1), and hence are quite "bumpy." In Sec. II we detail the simulation methods employed in this work. The results are presented in Sec. III, and Sec. IV concludes the paper.

II. SIMULATION DETAILS

We performed constant-pressure constant-temperature Monte Carlo (*NpT*-MC) simulations of N_m bent-core molecules in a cuboidal or a cubic simulation cell with periodic boundary conditions applied [12]. The cuboidal cell was constrained to have a square cross section, i.e., the box dimensions were $L_{xy}\times L_{xy}\times L_z$. To check that the cuboidal simulation cell did not artificially stabilize untilted solid or smectic phases, we computed the pressure tensor, Π, given by,

$$\prod = \left(\frac{N_m k_B T}{V}\right)\mathbf{I} + \frac{1}{V}\sum_{i=1}^{N_m}\sum_{j>i}^{N_m}\sum_{k=1}^{N_s}\sum_{l=1}^{N_s}(\mathbf{r}_{ik}-\mathbf{r}_{jl})\mathbf{f}_{ijkl}, \qquad (3)$$

where $\mathbf{I}$ is the second-rank unit tensor, $\mathbf{f}_{ijkl}$ is the force between the kth sphere on the ith molecule and the lth sphere on the jth molecule, and $(\mathbf{r}_{ik}-\mathbf{r}_{jl})$ is the corresponding sphere-sphere separation vector. In particular, we confirmed that the off-diagonal elements of the pressure tensor fluctuate about zero, indicating the absence of any significant stresses which might otherwise favor the development of a tilted simulation cell. We note that in almost all simulation studies of bent-core liquid crystals to date, untilted simulation cells have been employed without any reported pathological effects [4–9]. In the case of crystalline phases, however, the simulation cell should strictly be able to tilt—as in the Parrinello-Rahman method [13,14]—but these phases are not of primary concern in the current study.

The following reduced units are defined in terms of the LJ interaction parameters: the reduced pressure, $p^*=p\sigma^3/\epsilon$; the reduced temperature, $T^*=k_BT/\epsilon$, where k_B is Boltzmann's constant; the reduced molecular number density, $\rho^*=N_m\sigma^3/V$, where V is the volume of the simulation cell.

One MC sweep consisted of one trial translation or one trial rotation per molecule, and a single volume move. The rotational moves were effected by the Barker-Watts method [12]. Volume moves were carried out by sampling ln V [12]; in the cuboidal-cell simulations, the dimension to be scaled (L_{xy} or L_z) was chosen at random. All maximum displacement parameters were adjusted to give respective acceptance ratios of 50%. In general, we found that the equilibration of the simulations was sluggish, requiring $\sim 10^6$ MC sweeps; after equilibration we carried out production runs of comparable length.

Isotropic and nematic phases were simulated in a cubic simulation cell, whilst smectic phases were accommodated in a cuboidal simulation cell. In all simulations, the total number of molecules was $N_m=400$. In the simulations with a cuboidal cell, the molecules were distributed amongst four smectic layers of 100 each, with the layer normals aligned initially along the z direction. Although no constraints were applied to maintain the orientations of the smectic layer normals along the z direction, a visualization of simulation snapshots showed that they did not rotate significantly during the course of the simulations.

The global orientational ordering of the model molecules was assumed to involve preferential ordering of a set of molecular axes, defined as follows. The unit vectors $\hat{\mathbf{e}}_1$ and $\hat{\mathbf{e}}_2$ in Fig. 2 describe the orientations of the two "arms" of the molecule, with $\hat{\mathbf{e}}_1\cdot\hat{\mathbf{e}}_2=-\cos\gamma$. The molecular frame is defined by three orthonormal vectors given by

$$\hat{\mathbf{a}} = \frac{\hat{\mathbf{e}}_1 - \hat{\mathbf{e}}_2}{|\hat{\mathbf{e}}_1 - \hat{\mathbf{e}}_2|}, \qquad (4)$$

$$\hat{\mathbf{b}} = \frac{\hat{\mathbf{e}}_1 + \hat{\mathbf{e}}_2}{|\hat{\mathbf{e}}_1 + \hat{\mathbf{e}}_2|}, \qquad (5)$$

$$\hat{\mathbf{c}} = \hat{\mathbf{a}} \times \hat{\mathbf{b}}. \qquad (6)$$

Uniaxial and biaxial ordering of the molecules are described by the parameters Q^2_{00} and Q^2_{22} given by

$$Q^2_{00} = \frac{1}{2}(3\cos^2\theta - 1), \qquad (7)$$

$$Q^2_{22} = \frac{1}{2}(1+\cos^2\theta)\cos 2\phi\cos 2\psi - \cos\theta\sin 2\phi\sin 2\psi, \qquad (8)$$

where (ϕ,θ,ψ) are the Euler angles in the rotation matrix mapping the molecular frame defined by Eqs. (4)–(6) to the laboratory frame [15]. To identify the laboratory frame, we take the director of the most aligned molecular axis to define the laboratory Z axis. The director of the second-most aligned molecular axis is taken to be the laboratory Y axis, and the X axis is orthogonal to Y and Z. With this convention, $Q^2_{00}=1$ and $Q^2_{22}=0$ denote a phase with perfect uniaxial orientational ordering, whilst $Q^2_{00}=1$ and $Q^2_{22}=1$ describe a phase with perfect biaxial orientational ordering. In the simulations, the directors and order parameters were obtained by diagonalizing the order tensors [16]

$$\mathbf{Q}_{aa} = \frac{1}{2N_m}\sum_{i=1}^{N_m}(3\hat{\mathbf{a}}_i\hat{\mathbf{a}}_i - \mathbf{I}), \tag{9}$$

where $\mathbf{I}$ is the second-rank unit tensor; corresponding definitions hold for $\mathbf{Q}_{bb}$ and $\mathbf{Q}_{cc}$. Diagonalization of each tensor in turn yields the eigenvalues $\lambda^+ \geqslant \lambda^0 \geqslant \lambda^-$, and the corresponding orthonormal eigenvectors, $\hat{\mathbf{n}}^+$, $\hat{\mathbf{n}}^0$, and $\hat{\mathbf{n}}^-$. The molecular axis with the largest λ^+ is identified as the z axis of the molecular frame, and the corresponding eigenvector (director) defines the laboratory Z axis ($\mathbf{Z}$). The molecular axis with the second-largest λ^+ is the y axis of the molecular frame, and the corresponding eigenvector (director) defines the laboratory Y axis ($\mathbf{Y}$). The molecular axis with the lowest λ^+ is taken to be the x axis of the molecular frame, and the laboratory X axis ($\mathbf{X}$) is orthogonal to $\mathbf{Y}$ and $\mathbf{Z}$. With these assignments, the order parameters in Eqs. (7) and (8) are equal to

$$Q_{00}^2 = \mathbf{Z}\cdot\mathbf{Q}_{zz}\cdot\mathbf{Z}, \tag{10}$$

$$Q_{22}^2 = \frac{1}{3}(\mathbf{X}\cdot\mathbf{Q}_{xx}\cdot\mathbf{X} + \mathbf{Y}\cdot\mathbf{Q}_{yy}\cdot\mathbf{Y} - \mathbf{X}\cdot\mathbf{Q}_{yy}\cdot\mathbf{X} - \mathbf{Y}\cdot\mathbf{Q}_{xx}\cdot\mathbf{Y}). \tag{11}$$

We note that finite-size errors are apparent in the order parameters calculated by diagonalizing order tensors; in the isotropic phase the errors are $\mathcal{O}(1/\sqrt{N_m})$, while in orientationally ordered phases, the errors are $\mathcal{O}(1/N_m)$ [17].

In all cases, the full radial distribution function, $g(r)$, was computed, but to help characterize smectic phases in a cuboidal simulation cell, the correlations between molecules in the same smectic layer were quantified by calculating the in-layer (two-dimensional) radial distribution function, $g_{xy}(r)$. This latter function is defined by

$$g_{xy}(r) = \left\langle \frac{L_{xy}^2}{2\pi r N_l^2}\sum_{i=1}^{N_l}\sum_{j\neq i}^{N_l}\delta(|\mathbf{r}_i - \mathbf{r}_j| - r)\right\rangle, \tag{12}$$

where $N_l = 100$ is the number of molecules within the layer, and $\mathbf{r}_i$ is the position vector of the apical sphere on the ith molecule.

The average tilt angle Φ between the molecular a axes and the smectic-layer normal was computed using

$$\cos\Phi = \frac{1}{N_m}\sum_{i=1}^{N_m}|\hat{\mathbf{a}}_i\cdot\hat{\mathbf{l}}|, \tag{13}$$

where $\hat{\mathbf{l}}$ is the layer normal, which we took to be the z axis of the simulation cell, since in simulation snapshots we could observe no significant rotation of $\hat{\mathbf{l}}$ during the course of the calculations.

For each system considered, we carried out sequences of simulations starting from *untilted* configurations on simple close-packed lattices in cuboidal simulation cells, with reduced densities of either $\rho^* = 0.14$ or $\rho^* = 0.15$. The reason for selecting untilted starting points was to ensure that molecular tilt developed spontaneously. After equilibration, we raised the temperature until we detected a transition to a homogeneous fluid phase (isotropic or nematic). We then switched over to a cubic simulation cell and carried out some cooling runs to confirm the existence of a transition, as well as performing some further heating runs to map out the high-temperature behavior. With $\gamma = 40°$, we carried out separate runs starting from perfectly ordered ferroelectric and antiferroelectric configurations, in order to detect any differences in the relative mechanical stabilities of the two polarization states. In most cases, (anti)ferroelectric ordering did not persist for the duration of the runs due to the smectic-layer polarizations reorienting in random directions.

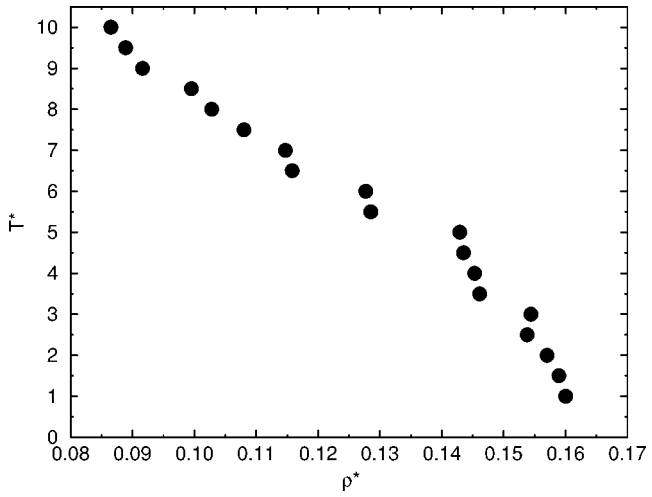

FIG. 3. The equation of state (temperature as a function of density) for CLJMs with external bond angle $\gamma = 0°$, along an isobar with $p^* = 4.0$.

III. RESULTS

A. $\gamma = 0°$

The equation of state of linear ($\gamma = 0°$) CLJMs along an isobar with $p^* = 4.0$ is shown in Fig. 3. Snapshots of the system at $T^* = 2.0$ shown in Figs. 4(a) and 4(b) clearly show crystalline ordering within the layers, and that the layers are tilted with respect to the layer normal. This kind of tilt has been demonstrated in simulations of solid-phase semiflexible chains made up of six spheres interacting via a truncated-and-shifted Lennard-Jones potential [18], in the calculations of Paolini *et al.* using a soft-sphere model [10], and in the simulations of three- and five-LJ-sphere linear molecules by Galindo *et al.* [11]. In our calculations, the average tilt angle of the molecules with respect to the layer normal—which develops spontaneously—is $\Phi \simeq 35°$, indicating the approximately close-packed interdigitation of the spheres within each layer. This tilt angle is comparable to the range of angles observed in experiments, this being between 25° and 35° [19,20], but in our simulations there is no global tilt direction. Our interest is not in the crystalline phases, but we note that a truly long-range ordered solid phase seems to be the thermodynamically stable state at temperatures $T^* \leqslant 3.0$. In these simulations carried out in the cuboidal simulation cell, the off-diagonal elements of the stress tensor fluctuated about zero, albeit sluggishly. Unsurprisingly, the worst

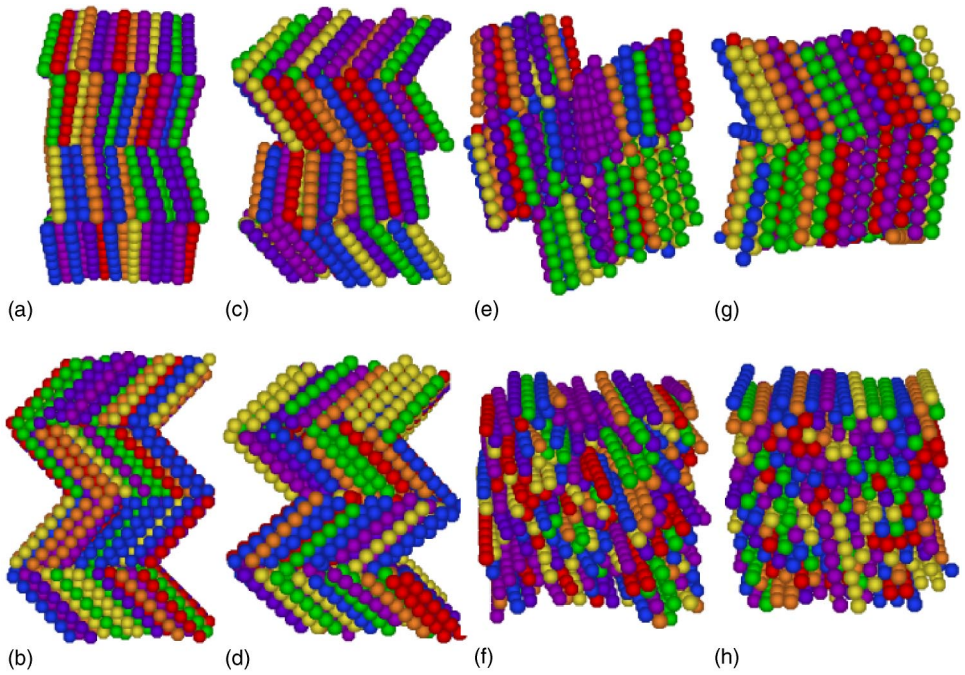

FIG. 4. (Color online) Snapshots from simulations of CLJMs with $\gamma=0°$, along an isobar with $p^*=4.0$: (a) and (b) crystalline phase at $T^*=2.0$ (cuboidal cell); (c) and (d) tilted smectic-*B* phase at $T^*=4.0$ (cuboidal cell); (e) and (f) untilted smectic *A* at $T^*=6.0$ (cubic cell); (g) and (h) tilted smectic-*B* phase at $T^*=4.0$ (cubic cell).

case was the low-temperature crystalline phase ($T^* \leqslant 3.0$) in which the root-mean-square fluctuations of Π_{xy}, Π_{xz}, and Π_{yz} were as high as $0.5\epsilon/\sigma^3$. We put this down to the fact that the simulation cell comprises only four tilted layers, leading to large statistical fluctuations. Our simulation results suggest that the uniformly tilted (synclinic) crystalline phase is not strongly favored over a phase with some disorder in the tilt directions. With regard to this question, we note that a similar situation holds in solid phases of hard dumbbell molecules [21], and in two-dimensional systems of hard-disk dimers [22]. It would be interesting to study further the possible crystalline phases of CLJMs, particularly in light of current research activity in polymorphism.

The low-temperature phase is stable up to a temperature $T^*=3.0$, above which it undergoes a crossover to a state which persists over the temperature range $3.5 \leqslant T^* \leqslant 5.0$, as evidenced by the distinct branch in the equation of state shown in Fig. 3; snapshots of this phase at $T^*=4.0$ obtained by heating from the crystalline phase are shown in Figs. 4(c) and 4(d). In an attempt to assess whether this state is metastable, a well-equilibrated untilted smectic-*A* phase at $p^*=4.0$ and $T^*=6.0$ ($\rho^*=0.128$) in a cubic simulation cell (see below) was cooled to $T^*=4.0$; snapshots of the untilted smectic-*A* phase at $T^*=6.0$ are shown in Figs. 4(e) and 4(f). Upon cooling, the final equilibrium density was $\rho^*=0.147$, which corresponds to the same branch of the equation of state obtained from the heating run; snapshots of this final state are shown in Figs. 4(g) and 4(h). Note that the tilt has been re-established spontaneously, and that the short-range ordering within the layer [shown in Fig. 4(h)] is hexagonal; there does not appear to be any crystalline long-range order. Without absolute free-energy calculations it is unclear whether these structures in the temperature range $3.5 \leqslant T^* \leqslant 5.0$ are representative of a true thermodynamically stable state. However, the distinct branch of the equation of state shows that this phase is at least mechanically stable, and on the basis of the structural properties indicated in Fig. 4, we tentatively assign this as a tilted smectic-*B* phase (since the in-layer short-range ordering is hexagonal).

Continuing along the isobar, we observe an *untilted* paraelectric smectic phase at temperatures of $T^*=5.5$ and 6.0, followed by a uniaxial nematic phase in the range $6.5 \leqslant T^* \leqslant 8.5$, and finally the isotropic phase at $T^* \geqslant 9.0$. The in-layer structure of the untilted smectic shown in Fig. 4(f) clearly exhibits only short-range ordering, and hence this is a smectic *A*.

In Fig. 5, the nematic order parameter Q_{00}^2 is shown as a function of temperature along the isobar with $p^*=4.0$. The crossover from tilted smectic and crystalline phases is clearly visible at $T^* \leqslant 5.0$. The tilted phases exhibit smaller values of Q_{00}^2 than does the nematic phase because the layers are not tilted in the same direction. The nematic-isotropic phase

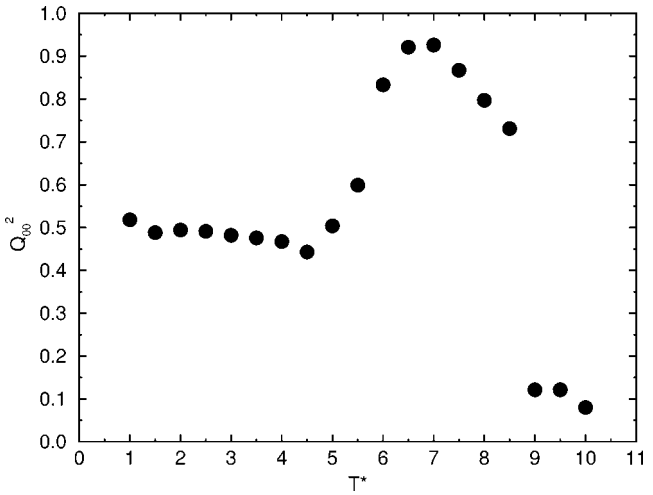

FIG. 5. The order parameter Q_{00}^2 as a function of temperature for CLJMs with external bond angle $\gamma=0°$, along an isobar with $p^*=4.0$.

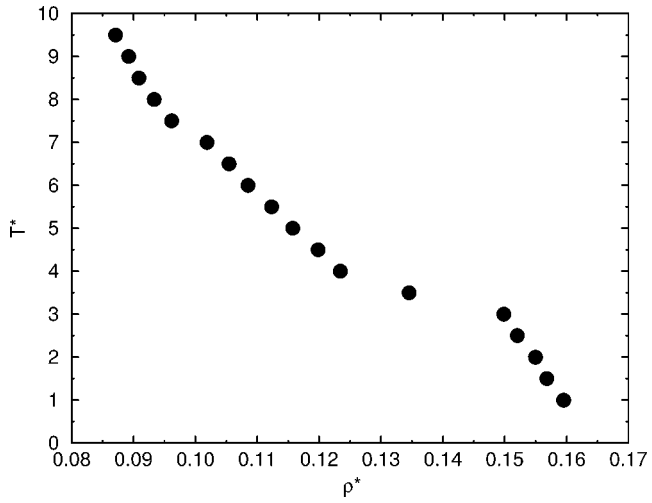

FIG. 6. Equation of state (temperature as a function of density) for CLJMs with external bond angle $\gamma=20°$, along an isobar with $p^*=4.0$.

transition is signaled by the drop in Q_{00}^2 between $T^*=8.5$ and 9.0.

With the exception of the tilted smectic-*B* phase ($3.5 \leqslant T^* \leqslant 5.0$), the phase behavior of CLJMs with $\gamma=0°$ is typical of cylindrically symmetric molecules with aspect ratios in the region of 10:1 [10].

B. $\gamma=20°$

The equation of state for CJLMs with $\gamma=20°$ along an isobar with $p^*=4.0$ is shown in Fig. 6. Three branches are apparent in the equation of state in the temperature ranges $T^* \leqslant 3.0$, $4.0 \leqslant T^* \leqslant 7.0$, and $T^* \geqslant 7.5$. The simulation at $T^*=3.5$ did not converge onto one of the main branches of the equation of state; the simulation configuration looks very much like the herring-bone structure shown in Figs. 4(c) and 4(d), and may represent a metastable state.

A snapshot from the simulation at $T^*=3.0$ is shown in Fig. 7(a). Clearly, the molecules are tilted within the layers; the average tilt angle with respect to the layer normal is $\Phi \simeq 35°$. In addition, the polarizations within the layer remain intact. The biaxial order parameter, Q_{22}^2, and the bulk polarization, $P \propto |\Sigma_{i=1}^{N_m} \hat{\mathbf{b}}_i \cdot \hat{\mathbf{n}}_b^+|$, where $\hat{\mathbf{n}}_b^+$ is the director of the molecular *b* axes, were seen to decay even during the lowest-temperature simulations, reflecting a low degree of correspondence between neighboring layers. Hence, this phase is superparaelectric, since it is the layer polarizations that are disordered, not the molecular orientations within the layer. From here on we will omit the descriptor "superparaelectric," since we have not found any stable ferroelectric or antiferroelectric smectic phases; the layer polarizations almost always rotated during the courses of the simulations to point in random directions. A detailed investigation of the in-layer structure at low temperatures suggests the existence of a smectic-*B* phase. Figure 8 shows the in-layer distribution function $g_{xy}(r)$ at two temperatures, $T^*=1.0$ and 3.0. At both temperatures, the second peak in $g_{xy}(r)$ is split, indicative of short-range hexagonal ordering. Neither of these functions is entirely consistent with long-range hexagonal (crystalline) ordering, however, and at the higher temperature, in-layer positional order is almost undetectable beyond $r/\sigma \simeq 4$. We therefore tentatively assign the low-temperature branch of the equation of state as corresponding to a tilted smectic-*B* phase. The alternatives are crystalline, or crystalline smectic; clearly the former is ruled out by a casual glance at Fig. 7(a). The differences between a smectic *B* and a "crystalline smectic" are subtle [23]. In a crystalline smectic, the layers possess long-range positional order, and obviously bond-orientational order, whereas neighboring layers are not in correspondence. In a smectic *B*, the layers

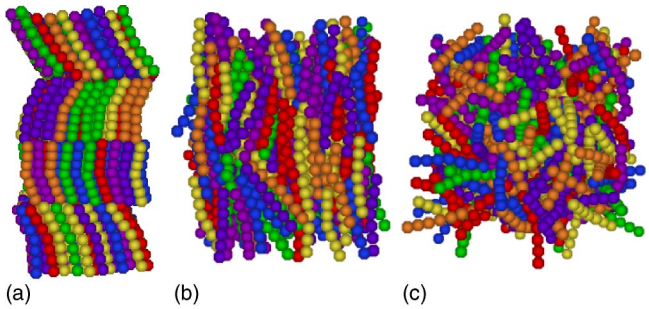

FIG. 7. (Color online) Snapshots from simulations of CLJMs with $\gamma=20°$, along an isobar with $p^*=4.0$: (a) tilted smectic-*B* phase at $T^*=3.0$ (cuboidal cell); (b) nematic phase at $T^*=5.0$ (cubic cell); (c) isotropic phase at $T^*=8.0$.

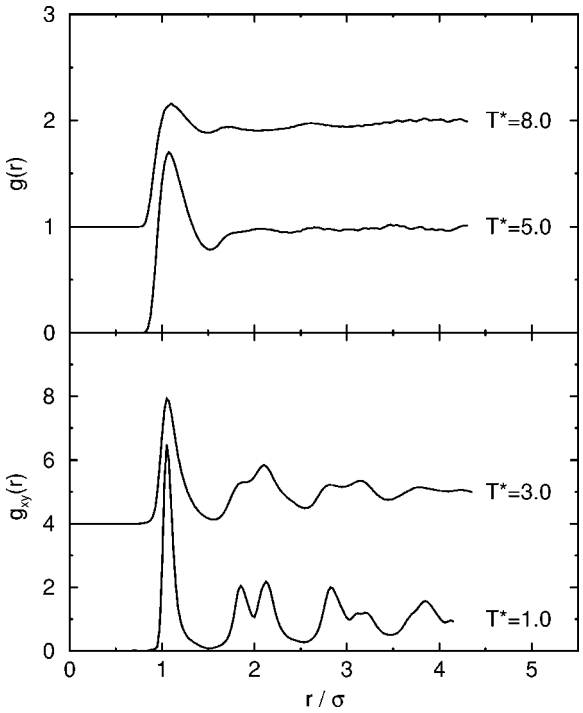

FIG. 8. Radial distribution functions for CLJMs with external bond angle $\gamma=20°$, along an isobar with $p^*=4.0$: (top) $g(r)$ in the isotropic phase at $T^*=8.0$ (upper), and in the uniaxial nematic phase at $T^*=5.0$ (lower) (functions are displaced by one unit for clarity); (bottom) in-layer radial distribution functions, $g_{xy}(r)$, in the tilted smectic-*B* phase at $T^*=3.0$ (upper) and 1.0 (lower) (functions are displaced by four units for clarity).

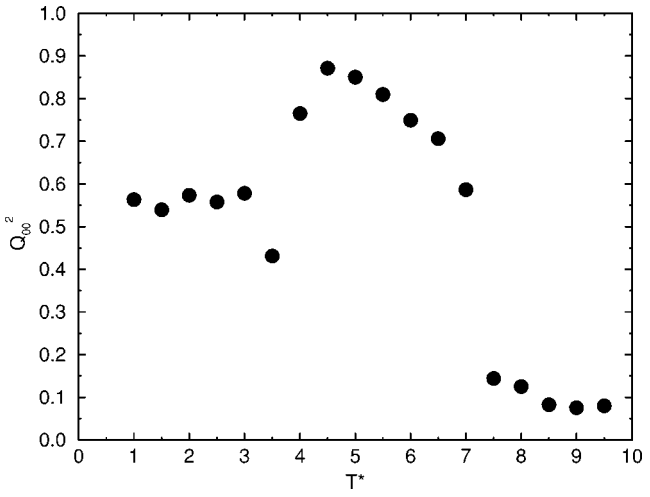

FIG. 9. The order parameter Q_{00}^2 as a function of temperature for CLJMs with external bond angle $\gamma=20°$, along an isobar with $p^*=4.0$.

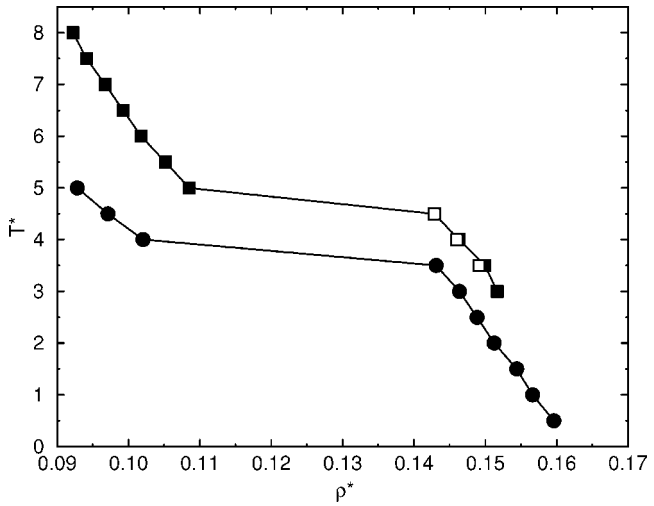

FIG. 10. The equation of state (temperature as a function of density) for CLJMs with external bond angle $\gamma=40°$, along isobars with $p^*=2.0$ (circles), and $p^*=4.0$ (squares). The filled and open symbols correspond to heating runs beginning from ferroelectric and antiferroelectric configurations, respectively (see text).

possess long-range bond-orientational order, but long-range crystalline order is destroyed by the presence of defects; typically, the positional order persists over a few hundred angstroms. Of course, in simulations with typical system sizes of $\sim 10^3$ molecules, it is almost impossible to make the distinction, because the long-range behavior of, say, $g_{xy}(r)$ is inaccessible. The snapshot in Fig. 7(a) is clearly not suggestive of a well-ordered crystalline phase, and hence we follow previous workers [7,8] and take the splitting of the second peak in $g_{xy}(r)$ as being indicative of a smectic-*B* phase.

The intermediate-temperature branch $(4.0 \leqslant T^* \leqslant 7.0)$ in the equation of state corresponds to a uniaxial nematic phase. A snapshot from the simulation at $T^*=5.0$ is shown in Fig. 7(b). The radial distribution function, $g(r)$, for this same state point is shown in Fig. 8, which reflects the complete lack of any long-range positional ordering. The nematic-isotropic transition occurs at $T^*=7.0-7.5$; a snapshot of the isotropic phase at $T^*=8.0$ is shown in Fig. 7(c), and the corresponding $g(r)$ is shown in Fig. 8.

In Fig. 9 we plot the uniaxial order parameter, Q_{00}^2, as a function of temperature along an isobar with $p^*=4.0$. The nematic-isotropic phase transition, signaled by a sharp drop in Q_{00}^2, is very clear at $T^*=7.0-7.5$. The smectic phase at $T^* \leqslant 3.0$ exhibits smaller values of Q_{00}^2 due to the *random* tilt directions of the layers [see Fig. 7(a)]. Once again, the simulation at $T^*=3.5$ is anomalous, and likely reflects some sort of metastable state.

C. $\gamma=40°$

Equations of state for CLJMs with $\gamma=40°$ along isobars with $p^*=2.0$ and 4.0 are shown in Fig. 10. For the high-density, low-temperature branch of the $p^*=4.0$ isobar, two sets of results are presented; one sequence starting from an untilted ferroelectric configuration, and the other from a corresponding antiferroelectric configuration. On the basis of these two sets of results, the equation of state does not give a clear indication of whether one polarization state is any more (mechanically) stable than the other. Indeed, during the course of the simulations along the high-density branches, it was observed that the biaxial order parameter, Q_{22}^2, and the polarization, $P \propto |\Sigma_{i=1}^{N_m} \hat{\mathbf{b}}_i \cdot \hat{\mathbf{n}}_b^+|$, were seen to decay as the individual layer polarizations became uncorrelated. We are therefore led to the conclusion that there is no strong thermodynamic driving force for the formation of either a ferroelectric or an antiferroelectric phase, and hence the superparaelectric configuration of layer polarizations emerges; in what follows we do not distinguish between simulations started from different configurations, since they give almost identical results. The individual layers in the layered phases did show significant molecular tilt; along both isobars, the tilt angle remained at a value of $\Phi \simeq 27°$.

Surprisingly, we found no evidence of transitions to nematic phases along either of the isobars. Instead, we observed some rather subtle changes in the structural features of the tilted smectic phases—as indicated by $g_{xy}(r)$—before they eventually "melted" in to the isotropic phase. This is illustrated in Figs. 11 and 12 for the isobars with $p^*=2.0$ and 4.0, respectively. Starting with the lower-pressure isobar (Fig. 11), the in-layer distribution functions for $T^*=1.5$ and 3.0 retain a split second peak, which is indicative of a smectic-*B* phase; this persists up to the transition to the isotropic phase, which at $p^*=2.0$ is found to occur at $T^*=3.5-4.0$. The results for the isobar with $p^*=4.0$ are more interesting. The in-layer distribution functions indicate smectic-*B* ordering at $T^*=3.0$, but smectic-*A* ordering at $T^*=4.5$. By performing several independent runs at $T^*=3.0$, we confirmed that the smectic-*A* ordering was reproducible. We reiterate that molecular tilt within the layers persisted in all of the smectic phases.

In Fig. 13 we show the variation of the uniaxial order parameter, Q_{00}^2, as a function temperature along isobars with $p^*=2.0$ and 4.0. The smectic-isotropic transition is clearly signaled by a drop in Q_{00}^2 at $T^*=3.5-4.0$ for $p^*=2.0$, and at $T^*=4.5-5.0$ for $p^*=4.0$.

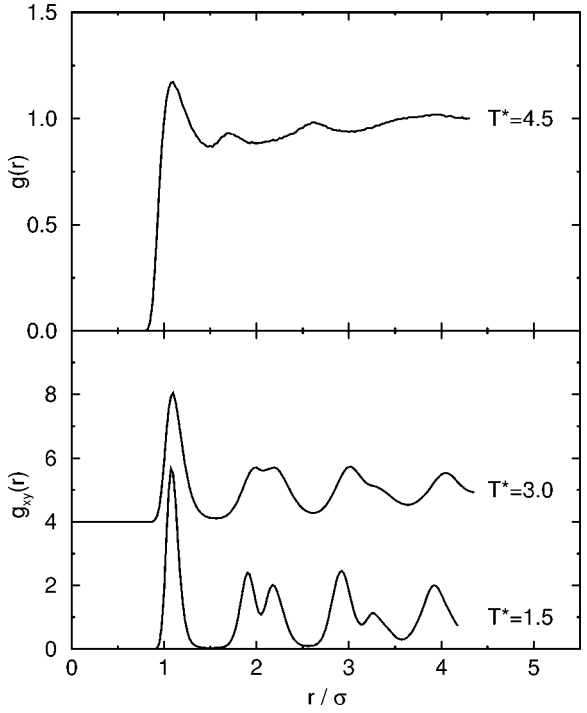

FIG. 11. Radial distribution functions for CLJMs with external bond angle $\gamma=40°$, along an isobar with $p^*=2.0$: (top) $g(r)$ in the isotropic phase at $T^*=4.5$; (bottom) in-layer radial distribution functions, $g_{xy}(r)$, in the tilted smectic-*B* phase at $T^*=3.0$ (upper) and $T^*=1.5$ (lower) (functions are displaced by four units for clarity).

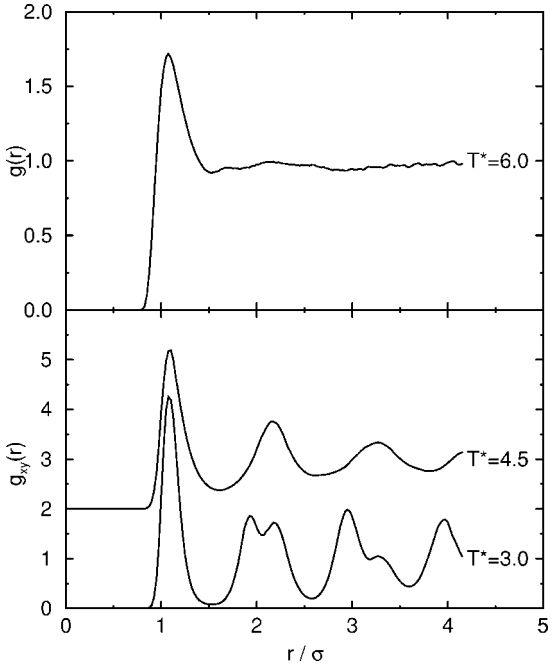

FIG. 12. Radial distribution functions for CLJMs with external bond angle $\gamma=40°$, along an isobar with $p^*=4.0$: (top) $g(r)$ in the isotropic phase at $T^*=6.0$; (bottom) in-layer radial distribution functions, $g_{xy}(r)$, in the tilted smectic-*A* phase at $T^*=4.5$ (upper), and in the tilted smectic-*B* phase at $T^*=3.0$ (bottom) (functions are displaced by two units for clarity).

IV. DISCUSSION

In this paper we have presented results from constant-pressure Monte Carlo computer simulations of model bent-core molecules (CLJMs) made up of seven Lennard-Jones spheres arranged to form a rigid "V"-shaped molecule with external bond angle γ. We have surveyed the phase behavior of CLJMs as a function of γ.

With $\gamma=0°$ (linear molecules), we find evidence for isotropic, nematic, untilted smectic-*A*, tilted smectic-*B*, and crystalline phases. The smectic-*B* and crystalline phases exhibit a molecular tilt of around 35° with respect to the layer normal, which confirms that, at least in this site-site model, tilted smectic phases are stabilized by a "close packing" of the spheres within a layer, as suggested by Xu *et al.* [9]. The observed phase behavior is in broad agreement with previously published work on linear molecules made up of 11 soft spheres (with repulsive interactions only) [10], with the exception of the tilted smectic-*B* phase. The existence of this phase demands further study, probably with the application of absolute free-energy calculations to confirm its thermodynamic (meta)stability. We note that the cuboidal simulation cells employed in this work may, in principle, artificially destabilize the synclinic crystalline phase, although no significant buildup of nonhydrostatic stresses was observed during the simulations.

For the system with $\gamma=20°$, we find isotropic, nematic, and tilted smectic-*B* phases. The range of stability of the uniaxial nematic phase is enhanced with respect to that in the $\gamma=0°$ system. In the smectic-*B* phase, the molecular tilt is in the region of 35° with respect to the layer normal.

With $\gamma=40°$, the nematic phase is no longer in evidence, the only phases we could find being isotropic and tilted smectic. At high pressure, the tilted smectic phase showed smectic-*A* ordering at high temperature, and smectic-*B* ordering at low temperature; the molecular tilt was around 27° with respect to the layer normal.

In none of these systems did we find evidence of truly chiral smectic phases, be they synclinic ferroelectric or anti-

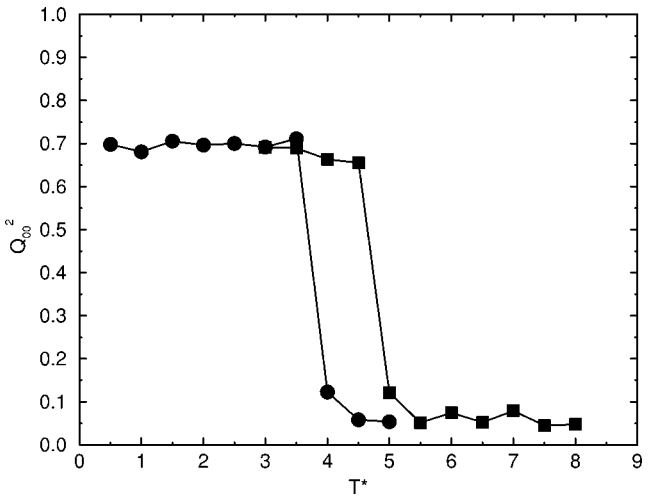

FIG. 13. Order parameter Q_{00}^2 as a function of temperature for CLJMs with external bond angle $\gamma=40°$, along isobars with $p^*=2.0$ (circles) and 4.0 (squares).

clinic antiferroelectric. In simulations of the $\gamma=40°$ system starting from untilted ferroelectric and antiferroelectric configurations, molecular tilt developed spontaneously, but global biaxiality did not persist for the duration of the runs. We note, however, that the range of values for the molecular tilt which developed spontaneously ($\Phi=27-35°$) compares favorably with typical experimental observations ($\Phi=25-35°$). Our molecular model is quite "bumpy," and it is interesting to speculate as to why tilt angles in the region of 30° are favored over more extreme angles. One possibility is that with a high degree of tilt, to take advantage of favorable attractive interactions, neighboring smectic layers would have to interdigitate to a greater extent; this would almost certainly reduce the configurational entropy of each molecule. It may therefore turn out that a tilt angle of $\sim 30°$ represents an optimum balance of energy and entropy. To explore this issue, one could envisage carrying absolute free-energy calculations for systems with different proscribed tilt angles.

Of course, the most significant question is whether the present molecular model has any relevance to real bent-core molecules. On the one hand, the model is only a very crude representation of what are undoubtedly very complex molecules. On the other hand, it does possess the essential molecular characteristics of bend, interactions, and "bumpiness;" with regard to this latter point, it is worth remembering that the aryl groups in a typical bent-core molecule are very bulky.

With regard to further work, we are currently carrying out simulations of closely related molecular models that possess true dipole moments and flexible tails. Of course, the dipolar interaction is likely to stabilize antiferroelectric phases [8], but the specific role of flexible tails in stabilizing or destabilizing tilted smectics is, as yet, uncertain. Tail groups are a common element in bent-core molecules, and so this is likely to be a fruitful avenue of research. The results of these studies will appear in future papers.

ACKNOWLEDGMENTS

This research was supported by the Engineering and Physical Sciences Research Council (GR/45727/01), through the provision of computer hardware, and a studentship to A. D. We are grateful to Dr. Matthew Glaser for useful correspondence.

[1] T. Niori, T. Sekine, J. Watanabe, T. Furukawa, and H. Takezoe, J. Mater. Chem. **7**, 1231 (1996).
[2] A. Jákli, S. Rauch, D. Lötzsch, and G. Heppke, Phys. Rev. E **57**, 6737 (1998).
[3] R. Macdonald, F. Kentischer, P. Warnick, and G. Heppke, Phys. Rev. Lett. **81**, 4408 (1998).
[4] P. J. Camp, M. P. Allen, and A. J. Masters, J. Chem. Phys. **111**, 9871 (1999).
[5] Y. Lansac, P. K. Maiti, N. A. Clark, and M. A. Glaser, Phys. Rev. E **67**, 011703 (2003).
[6] R. Memmer, Mol. Phys. **29**, 483 (2000).
[7] S. J. Johnston, R. J. Low, and M. P. Neal, Phys. Rev. E **65**, 051706 (2002).
[8] S. J. Johnston, R. J. Low, and M. P. Neal, Phys. Rev. E **66**, 061702 (2002).
[9] J. Xu, R. L. B. Selinger, J. V. Selinger, and R. Shashidhar, J. Chem. Phys. **115**, 4333 (2001).
[10] G. V. Paolini, G. Ciccotti, and M. Ferrario, Mol. Phys. **80**, 297 (1993).
[11] A. Galindo, C. Vega, E. Sanz, L. G. MacDowell, E. de Miguel, and F. J. Blas, J. Chem. Phys. **120**, 3957 (2003).
[12] M. P. Allen and D. J. Tildesley, *Computer Simulation of Liquids* (Clarendon, Oxford, 1987).
[13] M. Parrinello and A. Rahman, Phys. Rev. Lett. **45**, 1196 (1980).
[14] S. Yashonath and C. N. R. Rao, Mol. Phys. **54**, 245 (1985).
[15] H. Goldstein, *Classical Mechanics*, 2nd ed. (Addison-Wesley, London, 1980).
[16] *The Molecular Physics of Liquid Crystals*, edited by G. R. Luckhurst and G. W. Gray (Academic, New York, 1979).
[17] R. Eppenga and D. Frenkel, Mol. Phys. **52**, 1303 (1984).
[18] J. M. Polson and D. Frenkel, J. Chem. Phys. **109**, 318 (1998).
[19] S. Diele, S. Grande, H. Kruth, C. H. Lischka, G. Pelzl, W. Weissflog, and I. Wirth, Ferroelectrics **212**, 169 (1998).
[20] J. P. Bedel, J. C. Rouillon, J. P. Marcerou, M. Laguerre, M. F. Achard, and H. T. Nguyen, Liq. Cryst. **27**, 103 (2000).
[21] L. Vega, E. de Miguel, L. F. Rull, G. Jackson, and I. A. McLure, J. Chem. Phys. **96**, 2296 (1992).
[22] K. W. Wojciechowski, D. Frenkel, and A. C. Branka, Phys. Rev. Lett. **66**, 3168 (1993).
[23] P. G. de Gennes and J. Prost, *The Physics of Liquid Crystals*, 2nd ed. (Clarendon, Oxford, 1993).